Engineered Science
DOI: https://dx.doi.org/10.30919/es1495

Upcycling Waste Polyethylene Terephthalate Bottles into Eco-Friendly Filaments for Material Extrusion 3D Printing

Siriwan Pongsathit,[1] Peerapong Chanthot,[1, 3] Syang-Peng Rwei[2] and Cattaleeya Pattamaprom[1,*]

Abstract

In this study, waste polyethylene terephthalate (PET) drinking water bottles were upcycled into 3D-printing filaments to reduce the carbon footprint of a material extrusion process. The potential improvement in recycled PET (R-PET) properties was investigated using two reactive additives: a multifunctional chain extender (CE) and a peroxide free-radical initiator. It was found that both neat and modified R-PET filaments with the lowest additive content could be printed to 100% completion at a lower temperature of 250 ℃ compared to virgin PET (V-PET) filament, which required 260 ºC. CE modification enhanced the melt strength, evidenced by a higher low-frequency storage modulus (G'), and provided stable filament dimensions. However, the 3D-printed specimens from CE-modified R-PET exhibited poorer tensile toughness (0.67 MPa) and greater warpage (3°) compared to those made from neat R-PET (1.0 MPa and 2.30°). In contrast, filaments produced from peroxide-modified R-PET resulted in specimens with the highest tensile toughness and the lowest warpage, with an optimal peroxide content of 0.25 wt%. Higher printing temperature (270 ℃) and bed temperature (80 ℃) maximized tensile toughness to 2.2 MPa and resulted in a milder warpage angle of 1.5°.

Keywords: Upcycling; Recycled polyethylene terephthalate; 3D printing, Material extrusion; Filament.
Received: 07 March 2024; Revised: 03 October 2024; Accepted: 05 October 2024.
Article type: Research article.

1. Introduction

3D printing, or additive manufacturing, is one of the fast-growing techniques embraced by several industries. It can fabricate physical objects from a digital file by successive addition of material. Compared to traditional processes, 3D printing offers significant advantages, such as the ability to construct complex, customized structures with minimal waste. [1,2] Thus far, many plastic materials have been commonly used in material extrusion 3D printing, where the popular ones include polylactic acid (PLA) and acrylonitrile butadiene styrene (ABS).[3,4] Due to a stronger concern about natural resource scarcity and more severe environmental problems, sustainable production has become an urgent requirement in all manufacturing sectors including 3D printing. One effective way to reduce the carbon footprint of 3D printing is by utilizing recycled materials. So far, the recycled materials investigated as 3D-printing filaments include recycled polyethylene terephthalate (R-PET),[3] recycled polypropylene (R-PP),[2-6] recycled high-density polyethylene (R-HDPE),[7-10] recycled polylactic acid (R-PLA),[11-13] recycled acrylonitrile butadiene styrene (R-ABS),[14] recycled high-impact polystyrene (R-HIPS),[15] and recycled polycarbonate (R-PC).[16] Among these, R-PET is of particular interest because millions of short-life PET drinking bottles are generated every day. However, these bottles cannot be easily recycled into new drinking bottles due to hygienic concerns and severe degradation during reprocessing.[8] This degradation leads to lower molecular weight, viscosity, and melt strength,[17] as well as poorer mechanical and physical properties of final products.[11] A more effective way to utilize PET waste is by upcycling it into higher-value products. A chain extender (CE) can be used to restore its molecular weight, thereby improving its overall quality and suitability for various applications. CEs reportedly used in the literature include pyromellitic dianhydride (PMDA),[18,19] diisocyanates,[20] di-epoxides,[21] and acrylic multifunctional

[1] *Research Unit in Polymer Rheology and Processing, Department of Chemical Engineering, Faculty of Engineering, Thammasat School of Engineering, Thammasat University, Pathumthani 12120, Thailand*
[2] *Institute of Organic and Polymeric Materials, National Taipei University of Technology, Taipei, 10608, Taiwan*
[3] *Department of Chemical Engineering, Ubon Ratchathani University, Sathonlamark Road, Ubon Ratchathani, 34190, Thailand*
**Email::* cattalee@engr.tu.ac.th (C. Pattamaprom)

oligomers.[22-26] Among these, acrylic multifunctional oligomers have been the most widely investigated. They have been reported to connect chains, resulting in higher molecular weight, branching, and even crosslinking, which alter the rheological and thermal properties of R-PET.[22-25] Makkam *et al*. (2014) reported that 0.6% acrylic multifunctional CE increased the tensile strength of R-PET from 15 MPa to 25 MPa, with % elongation rising from 2.8% to 3.5%. However, this high CE content also resulted in a gel content of 27.8%.[23] Although there are several reports on the use of R-PET in various applications, its use in 3D printing has been limited. Thus far, there has been only one report on 3D printing of R-PET.[3] It was found that neat R-PET could not be fabricated into 3D-printing filament due to its low melt viscosity, while R-PET modified with 0.75 wt% PMDA chain extender required a very high printing temperature of 275 ºC and a high heated bed temperature of 120 ºC for continuous printing. Even then, the printed specimens did not achieve accurate dimensions, and their mechanical properties were not reported. As can be seen, R-PET filaments still have much room for improvement.

In this work, recycled PET retrieved from drinking water bottles is investigated for its potential as 3D printing filaments, where the molecular weight and molecular structure of R-PET were modified by using an acrylic multifunctional CE and a peroxide radical initiator. Their effects on the rheological, mechanical, thermal, and morphological properties of the obtained R-PET filaments were examined. The 3D printing performance of these filaments and the properties of the 3D printed products were investigated at different printing and heated-bed temperatures.

2. Experimental

2.1 Materials

The discarded PET drinking water bottles were collected from a local recycling facility in Thailand. The bottles were then cut and ground into small pieces. The CE used in this work was a commercial acrylic multifunctional oligomeric chain extender (Joncryl® ADR 4468) manufactured by BASF Co., Ltd. Peroxide used as a radical initiator was di-tert-butyl peroxide purchased from Sigma-Aldrich. V-PET used for property benchmarking was an InnoPlus SA135T grade (MFR = 245 g/10min) purchased from Thai PET Resin Co., Ltd., Thailand.

2.2 Preparation of 3D-printing filaments

In this work, the V-PET and R-PET 3D-printing filaments were fabricated by using a twin-screw extruder (Lab Tech Engineering Co., Ltd., Thailand) with a screw diameter of 16 mm and a die diameter of 1.75 mm. The temperature profile in the barrel was ramped from 200 ºC at the feed zone to 260 ºC at the die head. The screw speed was fixed at 60 rpm and the filament diameter was controlled within the range of 1.5 – 1.8 mm.

2.3 Fabrication of 3D-printed specimens

The 3D-printing filaments obtained in section 2.2 were printed into dumbbell-shaped specimens following ASTM D368 type IV by using a Prusa® material extrusion 3D printer (model Prusa I3 MK3S+). The printed specimens were fabricated with a rectilinear pattern. The infill percentage was set at 100% to attain the maximum achievable strength. The first and the latter layer heights were 0.21 mm and 0.14 mm, respectively, which are typical values for standard-quality printing. The printing temperatures were varied at 260 °C and 270 °C, while the printing bed temperature was varied at 60 °C and 80 °C. The printing speed and travel speed were fixed as 40 mm/s and 50 mm/s, respectively, which are typical values for printing PLA.

2.4 Characterization

2.4.1 Morphological study of filaments

The surfaces of all filaments and the side surface of 3D-printed specimens were observed using a digital microscope (Dino-Lite Premier AM-3013T) at 50x and 150x magnifications, respectively.

2.4.2 Fourier transform infrared spectroscopy (FTIR) of filaments

The FTIR analysis of filaments was performed by using an Attenuated Total Reflectance (ATR) mode on a Perkin Elmer spectrometer. The infrared absorbance spectra of the samples were obtained over the range of 4000 - 400 cm^{-1} at 4 cm^{-1} resolution.

2.4.3 Proton nuclear magnetic resonance spectroscopy (^{1}H-NMR) of filaments

^{1}H NMR spectra of the neat and modified R-PET were measured with Ascend TM 600/Avance III HD, manufactured by Bruker Japan Co., Ltd, where deuterated chloroform ($CDCl_3$) (the chemical shift of 7.28 ppm) was used as a standard solvent to dissolve each sample.

2.4.4 Thermal properties of filaments

Thermal characterization of all filaments was performed using a DSC250 (TA Instruments Discovery) differential scanning calorimeter. A standard aluminum crucible containing 8-10mg of the samples was used in all the experiments. The first heating from 25 °C to 300 °C was followed by a cooling down to 25 °C and a second heating up to 300 °C. The heating and cooling rates were set to 10 °C/min with a constant nitrogen flow rate of 50 mL/min. The percent crystallinity (%X_c) of R-PET was calculated using the following Eq. (1).

$$\%\text{Crystallinity} = \left(\frac{\Delta H_m - \Delta H_c}{\Delta H_f}\right) \times 100 \quad (1)$$

where ΔH_m and ΔH_c are the melting and cold crystallization enthalpies of the compounds, respectively. ΔH_f is the

reference melting enthalpy of 100% crystalline PET (140.1 J/kg).[27]

2.4.5 Rheological properties of filaments

In this work, the rheological properties were investigated by using an Anton-Paar (MCR-102) rheometer in the dynamic oscillation mode. The measurements were performed by using parallel-plate fixtures with a 25-mm diameter and 1-mm gap to determine the complex viscosity (η*), storage modulus (G'), and loss modulus (G'') of all filaments.

The rheological technique is commonly used by polymer rheologists to indicate differences in molecular weight and molecular architecture of polymers. The difference in polymer molecular weight could be observed through the difference in friction to flow, expressed in terms of complex viscosity. The low-frequency η* of polymer melts can be correlated with their molecular weight through the empirical 3.4-power law, [28] as well as through theoretical models based on reptation theory.[29,30] These models suggest that the low-frequency η* is roughly proportional to the 3.4-power of the polymer's molecular weight. In addition, the solid-like behavior of polymers is expressed by the value of G'. For ideal viscous liquids, the value of G' is very low, whereas a higher G' value indicates the presence of more solid-like structures. The presence of branched or crosslinked structures, as well as solid fillers, leads to a higher value of G'.[31,32]

2.4.6 Gel content of filaments

The filaments (0.5 g) were cut into small pieces and then immersed in trifluoroacetic acid or TFA (50 mL) and kept in the dark for 24 h. The undissolved fraction was filtered and dried in an air oven until a constant weight was reached (W_1). The gel content of R-PET was calculated from the ratio of the remaining weight of the undissolved fraction (W_1) to the initial sample weight (W_0) as shown in Eq. (2).

$$\% \text{ Gel content} = \frac{W_1}{W_0} \times 100 \quad (2)$$

2.4.7 Mechanical properties

The impact strength of the compression molded specimens was determined according to ASTM D4812 standard by using a pendulum impact-Izod Impact Tester (Unnotched Izod), ZwickRoell GmbH & Co. KG, Ulm, Germany. The samples were prepared by cutting filaments into small pieces, which were then compressed at 260 ºC for 10 minutes. The compressed samples were subsequently cut into a rectangular shape of 64 × 12.7 × 3.2 mm and kept at 25 ºC for 24 hours for stress relaxation before the test. Three specimens were tested for each sample, and the average value was reported along with the error bars showing the minimum and maximum values.

The tensile properties of 3D-printed specimens were determined according to ASTM D368 Type IV standard by using a universal tensile testing machine (Narin Instrument Co., Ltd., Thailand) with a load cell of 3 kN. The distance between the grips was set at 65 mm and the cross-head speed was 5 mm/min. The tensile toughness was calculated as the area under the stress-strain curve. Five specimens were tested for each sample, and the average value was reported along with the error bars showing the minimum and maximum values.

3. Results and discussion

In this work, the results are presented in 3 sections, starting by (1) introducing the filament processability and characteristics, followed by (2) the effect of additives and (3) printing parameters on the properties of 3D-printed specimens.

3.1 Filament processability and characteristics

In the filament production step, the output rate and screw speed were fixed at 5 kg/h and 60 rpm, respectively, at a fixed nip roll speed of 10 m/min. The resulting die stock temperature (T_{die}), % torque, die pressure (P_{die}), filament diameter, and surface morphologies are summarized in Table 1.

As can be seen, the fabrication of neat V-PET filament resulted in higher T_{die} and P_{die} than those of the neat R-PET filament expectedly due to its higher viscosity and molecular weight. For the modified R-PET filament, the addition of CE caused a dramatic increase in T_{die} and P_{die}, where the highest CE content (0.75 wt%) required a higher extruder temperature and a lower output rate to maintain the torque and die pressure levels below the maximum machine limit. Conversely, the production of peroxide-modified R-PET filament did not cause a significant increase in the % torque, T_{die}, and P_{die}. Nonetheless, their optimum nip roll speed was raised from 10 m/min to 13 m/min to avoid filament sagging due to the lower viscosity.

For the visual appearance of filaments, the filaments made from neat V-PET, neat R-PET, and R-PET modified with peroxide appeared to be similarly opaque, whereas the CE-modified R-PET filaments appeared to be more transparent. This implies that the CE-modified R-PET filaments possessed lower % crystallinity than other filaments. Additionally, the filament size of CE-modified R-PET was higher than those of other R-PET filaments, and the size increased with increasing CE content due to a higher degree of die swell, which implies a stronger elastic behavior.

Fourier transform infrared spectroscopy (FTIR) and Proton nuclear magnetic resonance spectroscopy (^{1}H-NMR) spectra were used to identify possible structural changes in the modified R-PET filaments, while macroscopic changes were examined through rheological properties and gel content, as discussed in a later section.

For CE-modified R-PET, the FTIR spectrum in Fig. 1a indicates that the addition of CE resulted in a slight increase in the peak intensity of C-O stretching (1041, 1091 and 1239

Table 1: The filament properties and morphologies taken by a digital microscope at 50x magnification.

Filament	Die stock temperature (T_{die}; ºC)	Torque (%)	Die pressure (P_{die}; bar)	Filament diameter ± S.D (mm)	Filament surface appearance (50x)
V-PET	253	62	99	1.55 mm ± 0.02	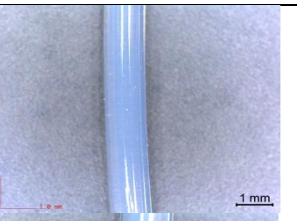
R-PET	251	73	78	1.59 mm ± 0.04	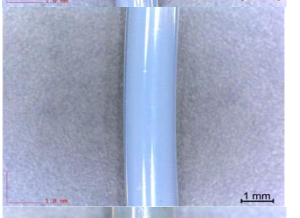
Chain extender 0.25 wt%	252	88	121	1.61 mm ± 0.03	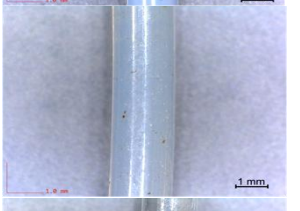
Chain extender 0.5 wt%	253	89	180	1.69 mm ± 0.02	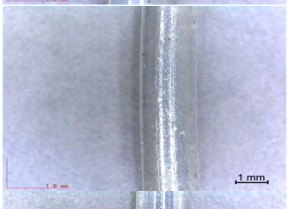
*Chain extender 0.75 wt%	262	89	132	1.75 mm ± 0.02	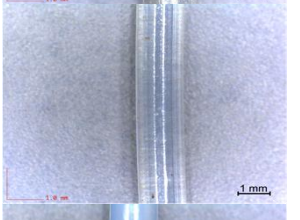
Peroxide 0.25 wt%	252	70	80	1.65 mm ± 0.07	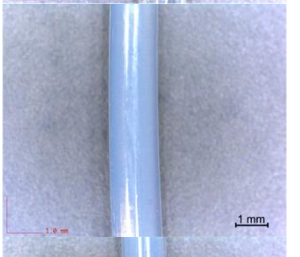
Peroxide 0.5 wt%	253	74	80	1.59 mm ± 0.05	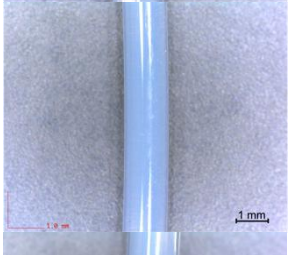
Peroxide 0.75 wt%	250	74	79	1.61 mm ± 0.06	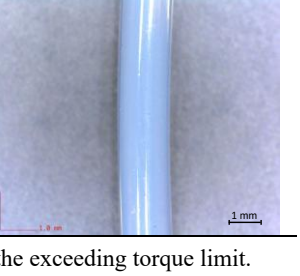

*Processed at a higher temperature profile and a lower output rate (4 kg/h) due to the exceeding torque limit.

cm^{-1}), CH_2 bending (1452 cm^{-1}), and C=O stretching (1718 cm^{-1}). As these functional groups are present in reacted CE, the increase in their peak intensity indicates a successful reaction of CE with R-PET. This corresponds to a slight increase in the ^{1}H-NMR chemical shifts of R–CH_2–R at 1.35 ppm. Moreover, the bonding of R-PET with CE is supported by a decrease in the chemical shift of the terminal CH_3 group in R-PET at 1.14 ppm (Fig. 1b). The proposed grafting reaction of CE with R-PET chains is shown in Fig. 2.

On the other hand, for peroxide-modified R-PET, the FTIR spectrum in Fig. 3a revealed a slight increase in C=C bending at 980 cm^{-1} and O-H bending at 1340 cm^{-1}, indicating chain scission in R-PET. Additionally, a slight decrease in -CH_2- bending at 1452 cm^{-1} indicates that peroxide led to hydrogen abstraction of the methylene group, potentially forming a grafted or branched structure. This is consistent with ^{1}H-NMR spectra in Fig. 3b, that the modified R-PET with peroxide showed a slightly decrease in the chemical shifts of R–CH_2–R (0.9 ppm), CH_2CH (1.45 ppm), and the terminal C-CH_3 (1.14 ppm).

The proposed chain scission and crosslinking mechanisms for peroxide-modified R-PET are illustrated in Fig. 4. This hypothesis is supported by rheological property analysis discussed in a later section.

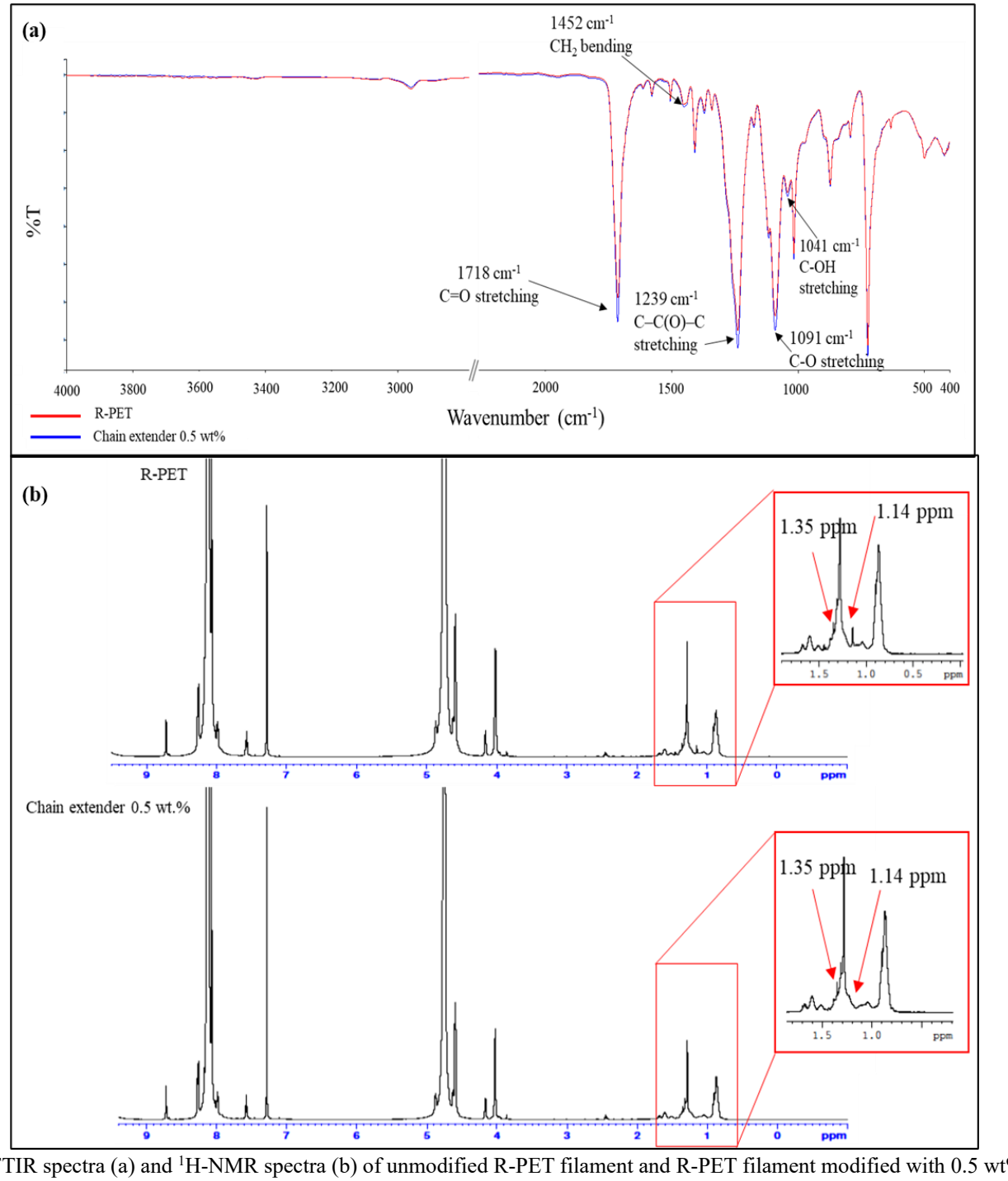

Fig. 1: FTIR spectra (a) and ^{1}H-NMR spectra (b) of unmodified R-PET filament and R-PET filament modified with 0.5 wt% CE.

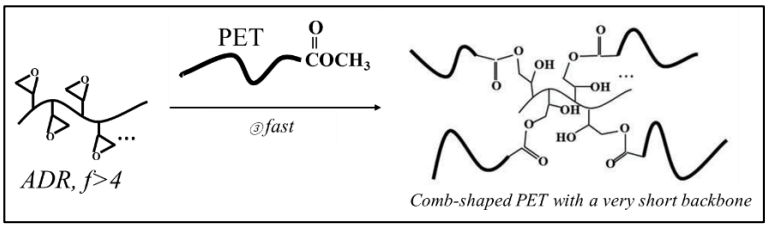

Fig. 2: Possible mechanism of PET reacted with a CE (Joncryl® ADR-4368).[20]

To draw a stronger conclusion on the structural changes, the rheological properties, thermal properties and gel content were determined and correlated in this section. The rheological parameters, such as complex viscosity (η*) and storage modulus (G'), can indicate macroscopic structural changes in polymers. Complex viscosity is strongly dependent on the molecular weight of the polymer, while G', which represents solid-like behavior, increases with the degree of branching and crosslinking within the polymer matrix. [31] Gel content is utilized to differentiate between the presence of crosslinked structures and branched structures. In Fig. 5a, the complex viscosity (η*) of extruded neat R-PET filament was significantly lower than that of unprocessed neat R-PET flake potentially due to chain scission induced by hydrolytic and thermal degradations under heat and shear.[25] With the addition of CE, η* and G' of R-PET systematically increased with increasing CE content (Fig. 5b and Fig. 6). This confirms the aforementioned implication of structural change into higher molecular weight, and branching (or crosslinking). Additionally, the gel content (Fig. 7) indicates that an excessively high CE content (0.75 wt%) induces a substantial amount of crosslinked gels in R-PET. This finding is consistent with the previously reported literatures.[23,24,26]

In the case of peroxide-treated R-PET, the peak intensity change in FTIR spectra discussed earlier suggested that peroxide-induced both chain scission and branching/crosslinking in R-PET. To confirm these structural changes, the rheological properties (η* and G'), which are

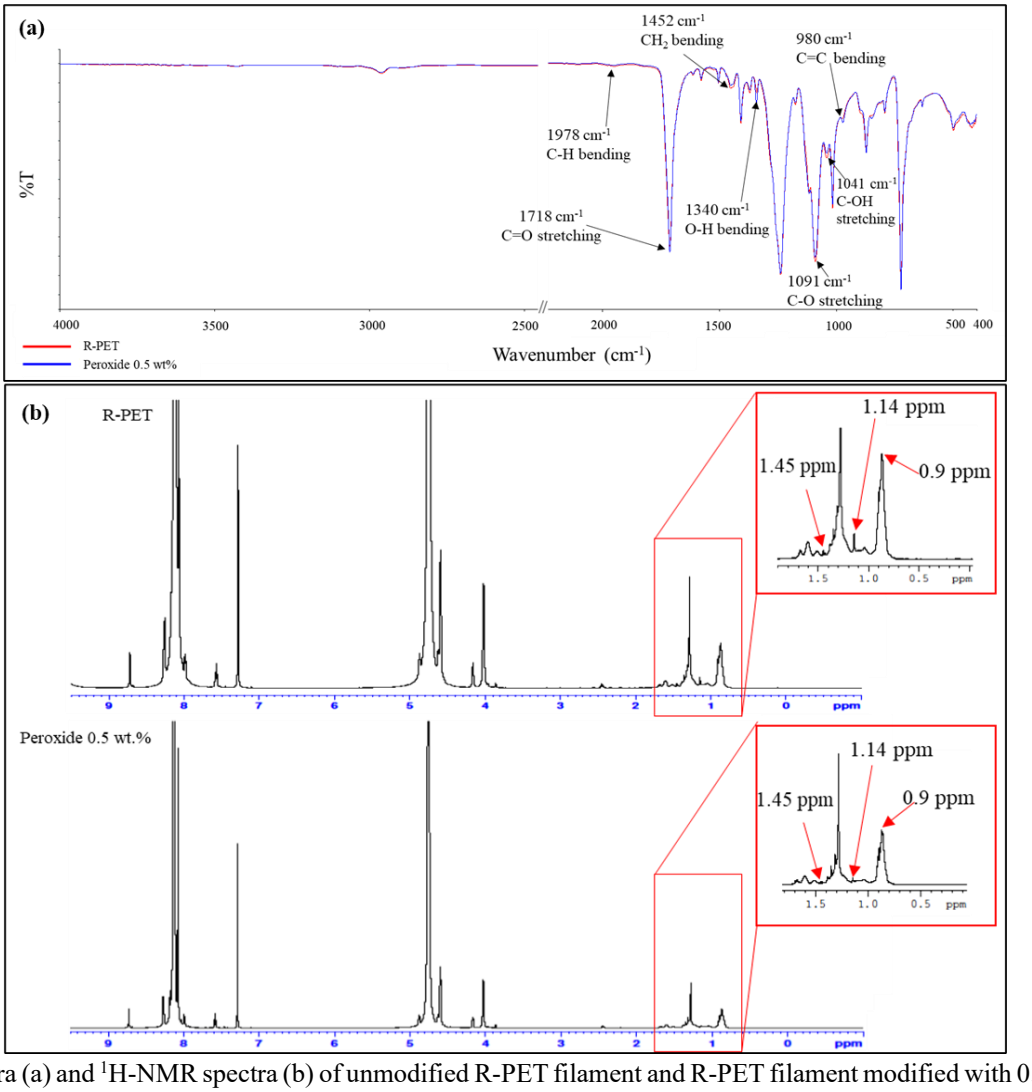

Fig. 3: FTIR spectra (a) and ^{1}H-NMR spectra (b) of unmodified R-PET filament and R-PET filament modified with 0.5 wt% peroxide.

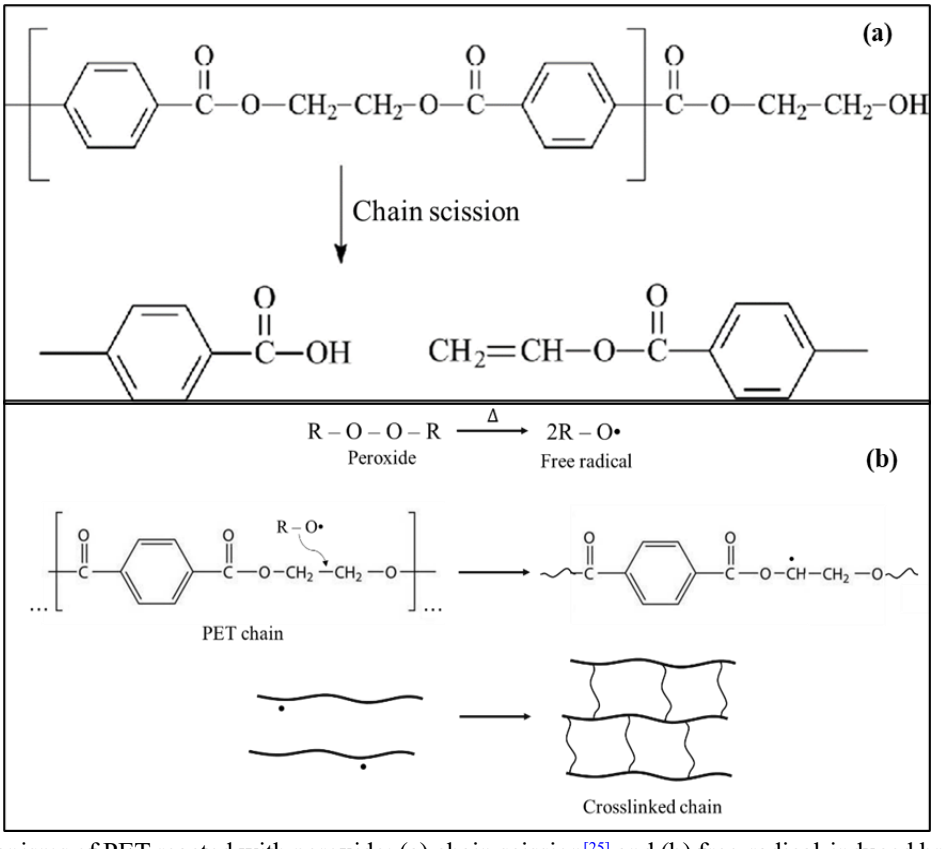

Fig. 4: Possible mechanisms of PET reacted with peroxide: (a) chain scission[25] and (b) free-radical-induced branching/crosslinking.

sensitive to molecular weight and molecular structure, can be used. For unfilled polymers, a higher value of low-frequency η* indicates an increase in molecular weight regardless of the molecular structure. Meanwhile, a higher G' in a relaxed state (no stress) suggests an increased degree of solid-like behavior due to the presence of branched or crosslinked structures. In Fig. 5c, the decreased η* of peroxide-treated R-PET indicates a reduction in molecular weight due to chain scission. Nevertheless, the unsystematic viscosity drop at higher peroxide contents suggests a competing effect between chain scission (lower η*) and branching/crosslinking (higher η*). Fig. 6 shows G' at different temperatures, where the G' values at high temperatures indicate solid-like behavior in a relaxed state (no stress). Therefore, the increasing high-temperature G' as peroxide content rises from 0 to 0.5 wt% suggests a higher degree of branching or crosslinking. In contrast, the G' values at high peroxide contents (0.5 - 0.75 wt%) do not change significantly, indicating a negligible change in the solid-like content. The gel content shown in Fig. 7 was used to assess the amount of crosslinking without the interfering effect of branching. A linear increase in gel content at higher peroxide dosages indicates a greater proportion of crosslinked structures.

All these test results collectively suggest that the structural changes in R-PET were predominantly due to chain scission, with minor competing effects from branching and crosslinking, where higher peroxide contents resulted in more crosslinking than branching. [33]

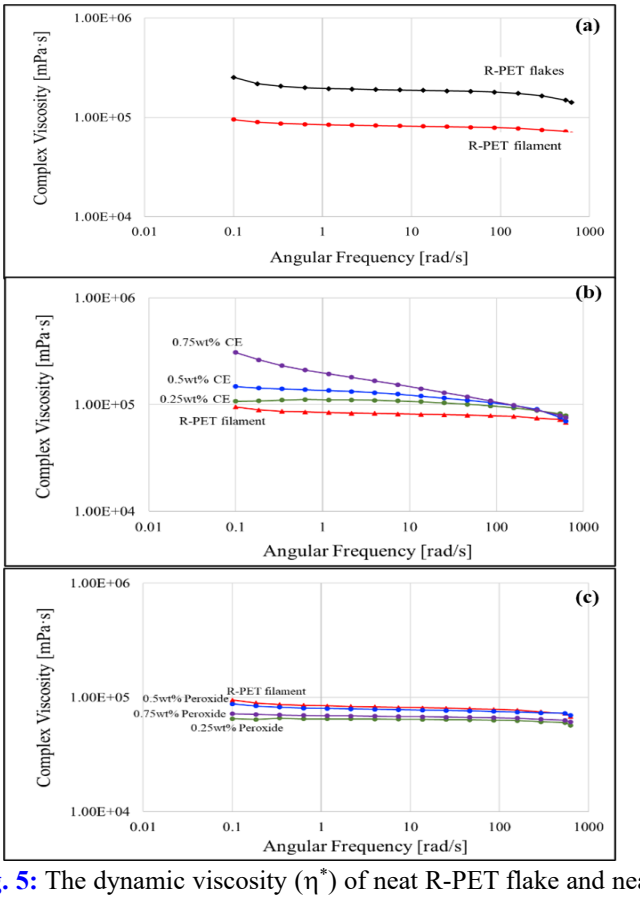

Fig. 5: The dynamic viscosity (η*) of neat R-PET flake and neat R-PET filament (a), R-PET modified with CE (b), and peroxide (c) at 260 ºC.

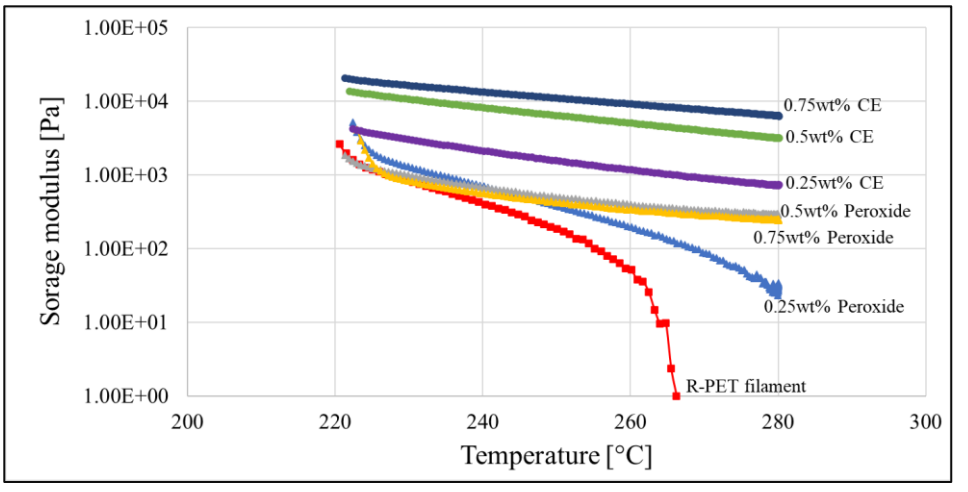

Fig. 6: The storage modulus (G') of all filaments measured by temperature sweep mode at the angular frequency of 100 s^{-1}.

The DSC thermograms of the V-PET, R-PET, and modified R-PET are shown in Fig. 8 and their thermal properties are summarized in Table 2. As can be seen, the addition of CE or peroxide into R-PET led to a lower T_g and T_m than the neat R-PET, where T_m reduction was more pronounced when adding CE, indicating poorer crystal quality. This is also supported by the more transparent filaments, the lower %crystallinity (Fig. 9), and the higher gel content (Fig. 7). This indicates that the higher CE content led to the lower degree of internal order by the formation of branching and crosslinking. For the case of peroxide, the $\%X_c$ of peroxide-treated R-PET was only slightly lower than neat R-PET with a slightly higher gel content.

The mechanical properties of the compressed filaments were examined in terms of impact strength, as shown in Fig. 10. As can be seen, unmodified R-PET exhibited the lowest impact strength due to degradation during reprocessing. The addition of either CE or peroxide enhanced the impact strength of R-PET to a comparable extent, although it remained slightly lower than that of V-PET.

3.2 The effect of CE and peroxide on 3D-printability and mechanical properties of 3D-printed parts

The lowest printable temperature of the filaments is defined as the temperature at which 3D-printed specimens could be successfully printed to 100% completion without interruption. In Fig. 11, the lowest printable temperature of filaments depended both on the melt viscosity and gel content. As can be seen, the neat R-PET and the modified R-PETs using the smallest additive content (0.25 wt%) could be printed at the lowest temperature of 250 ºC. When the additive content increased to 0.5 wt%, the lowest printable temperature increased to 260 ºC. At 0.75 wt% of peroxide-treated filament, the minimum printable temperature increased further to 270 ºC, while that of CE-treated one could not be printed even at the maximum machine printing temperature (295 ºC). The trend of higher printable temperature is strongly correlated with the gel content as reported in Fig. 7. Note that the lowest printable temperature of the V-PET filament (260 ºC) was higher than that of the unmodified R-PET filament (250 ºC) because of its higher melt viscosity. Our work reveals significant improvement over the only available literature on 3D-printing of R-PET filament,[3] which reported that unmodified R-PET could not be formed into 3D-printing filaments. In addition, their modification of R-PET with 0.75 wt% PMDA required a higher printing temperature of 275 ºC

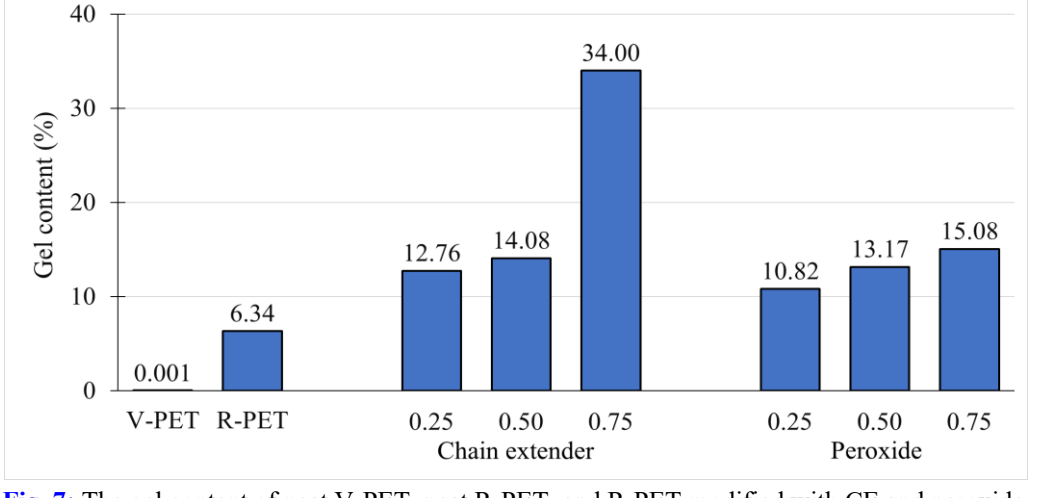

Fig. 7: The gel content of neat V-PET, neat R-PET, and R-PET modified with CE and peroxide.

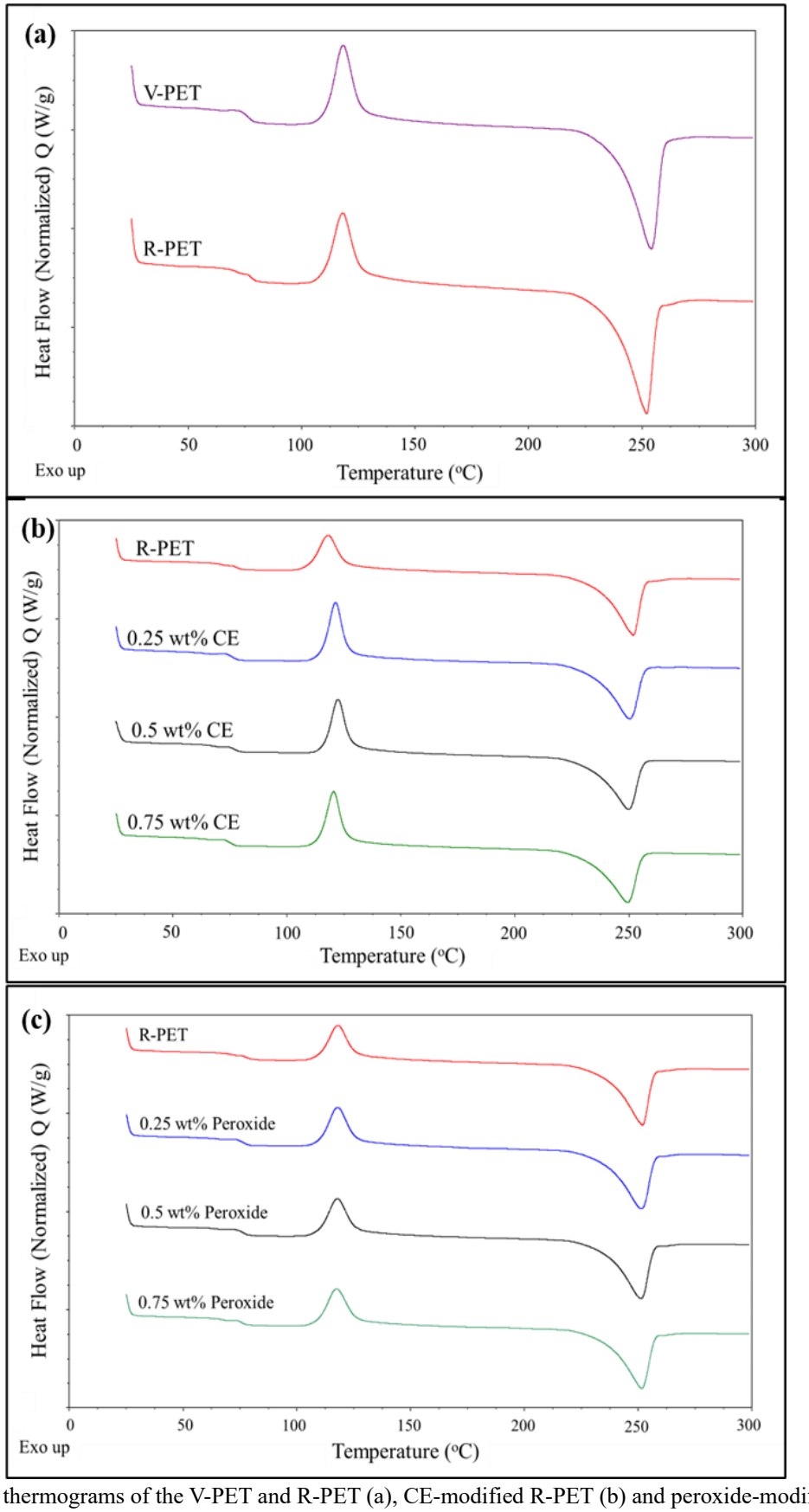

Fig. 8: The DSC thermograms of the V-PET and R-PET (a), CE-modified R-PET (b) and peroxide-modified R-PET (c).

and still could not produce a complete 3D-printed object.

The effects of R-PET modification on layer adhesion and interfacial morphology were observed through microscopic images taken by a Dino-Lite™ digital microscope at high magnification (150x), as shown in Table 3. The microscopic images of both unmodified and modified R-PETs at both 260

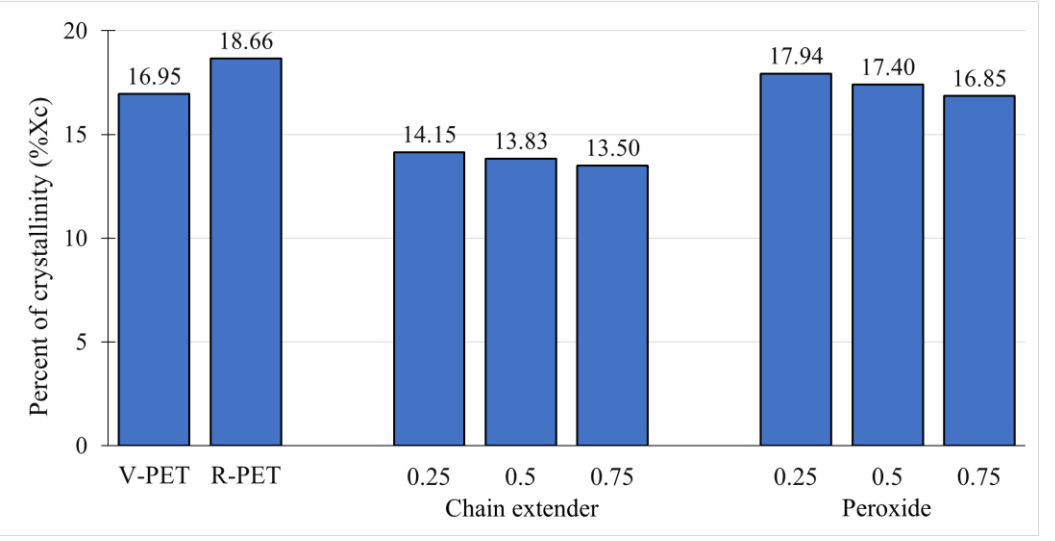

Fig. 9: The percent of crystallinity (%X_c) of neat V-PET, neat R-PET, and R-PET modified with multifunctional chain extender (CE) and peroxide.

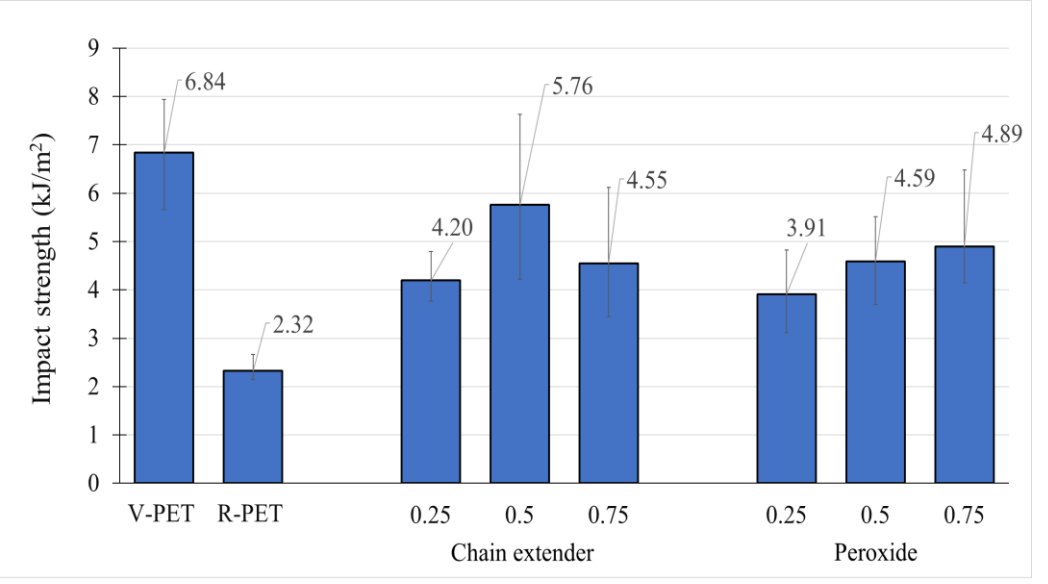

Fig. 10: Impact strength of all specimens obtained from compressed filaments at 260 ºC.

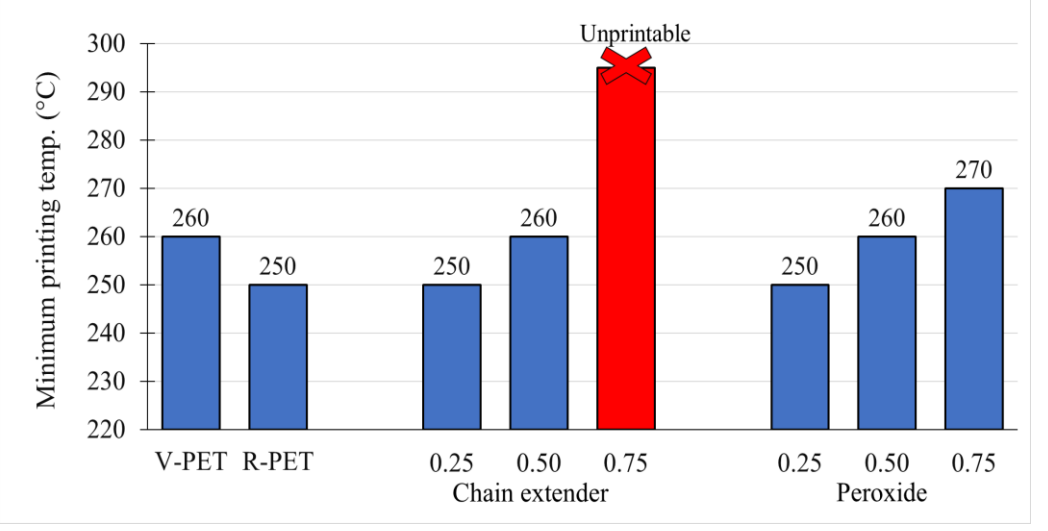

Fig. 11: The minimum printable temperature of all filaments.

Table 2: Thermal properties of neat and modified R-PET filaments.

Filaments		T_g (ºC)	T_m (ºC)	Degree of crystallinity (%)
Neat	V-PET	76.04	253.74	16.95
	R-PET	78.04	251.76	18.66
Chain extender	0.25 wt%	75.94	250.41	14.15
	0.5 wt%	76.78	250.06	13.83
	0.75 wt%	75.18	250.57	13.50
Peroxide	0.25 wt%	75.98	251.47	17.94
	0.5 wt%	76.04	251.23	17.40
	0.75 wt%	76.06	251.08	16.85

and 270 ºC show close layer stacking with no voids. As can be seen, the sharpness of layer boundaries depends on filament viscosity, as represented by η* in Fig. 5. Overall, the layer boundaries of all samples became more diffuse at the higher printing temperature, which indicates improved interlayer fusion resulting from lower filament viscosity. The layer morphology of R-PETs modified with CE and peroxide also clearly demonstrates the effect of filament viscosity. The CE-modified R-PETs exhibit sharper layer boundaries (indicating a lower degree of fusion) compared to the peroxide-modified R-PETs, consistent with their higher viscosity. Notably, the highest CE content (0.5 wt%) resulted in the sharpest layer boundary. Conversely, the 3D-printed layers of peroxide-treated R-PETs have more diffuse layer boundaries. This indicates a greater degree of layer fusion, which aligns with their lower η*. The highest degree of layer fusion was observed for filaments of R-PET treated with 0.25 wt% peroxide, corresponding to its lowest η*.

Unlike previous literature indicating that R-PET possessed too-low viscosity to be formed into 3D-printing filaments,[3] our study demonstrates that post-consumer R-PET filaments produced through our twin-screw extrusion process can be successfully manufactured with the toughness not significantly different from those of virgin PET (V-PET) (Fig. 12). This indicates that the filament preparation process strongly affects the properties of R-PET filaments. For the production of modification of R-PET filament, Unfortunately, the CE modification did not improve, and even lowered, the toughness and elongation at break of R-PET. This confirms the adverse effects of CE on mechanical properties previously reported.[24] Conversely, the addition of peroxide, particularly at the lowest concentration (0.25 wt%), resulted in significantly higher toughness compared to the CE-modified specimens, even surpassing that of the neat R-PET and V-PET specimens, despite similar gel contents.

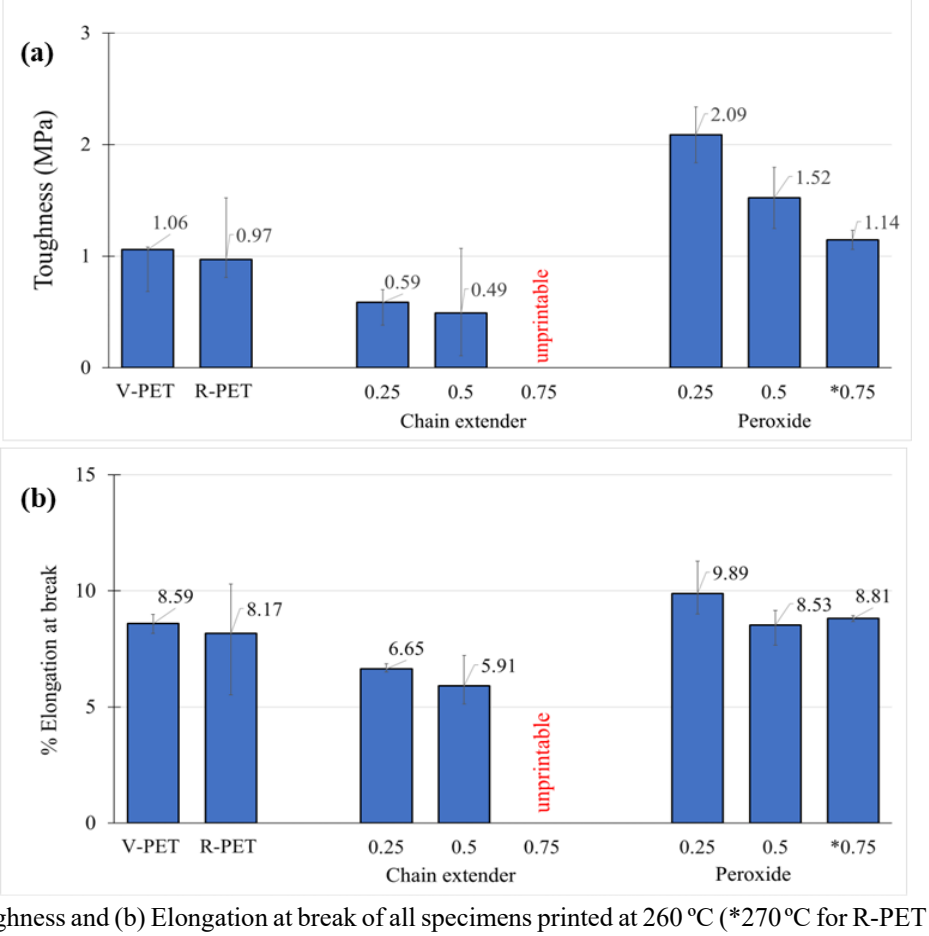

Fig. 12: (a) Tensile toughness and (b) Elongation at break of all specimens printed at 260 ºC (*270 ºC for R-PET with 0.75% peroxide) and the bed temperature of 60 ºC.

Table 3: Side surfaces of 3D-printed specimens revealing layer boundaries at 150x.

Specimens	Side surface of 3D-printed specimens at different printing temperatures (150x magnification)	
	260 ºC	270 ºC
R-PET	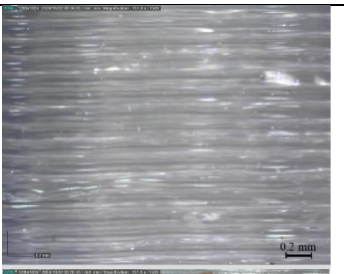	
CE 0.25		
CE 0.5		
Peroxide 0.25		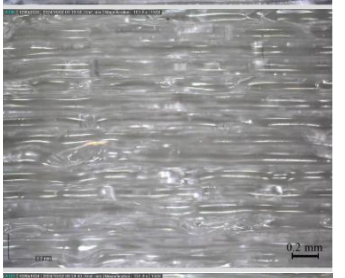
Peroxide 0.5	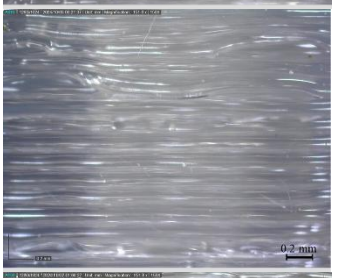	
Peroxide 0.75		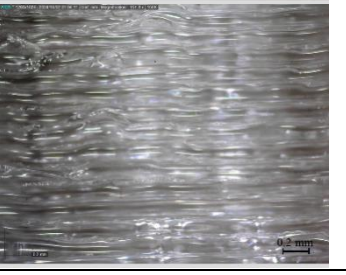

3.3 The effect of printing and bed temperatures on the specimen properties

In this part, the effect of printing and bed temperatures were investigated on the mechanical properties of 3D-printed specimens. Fig. 13 compares the effect of printing temperatures between 260 ºC and 270 ºC. It was found that the

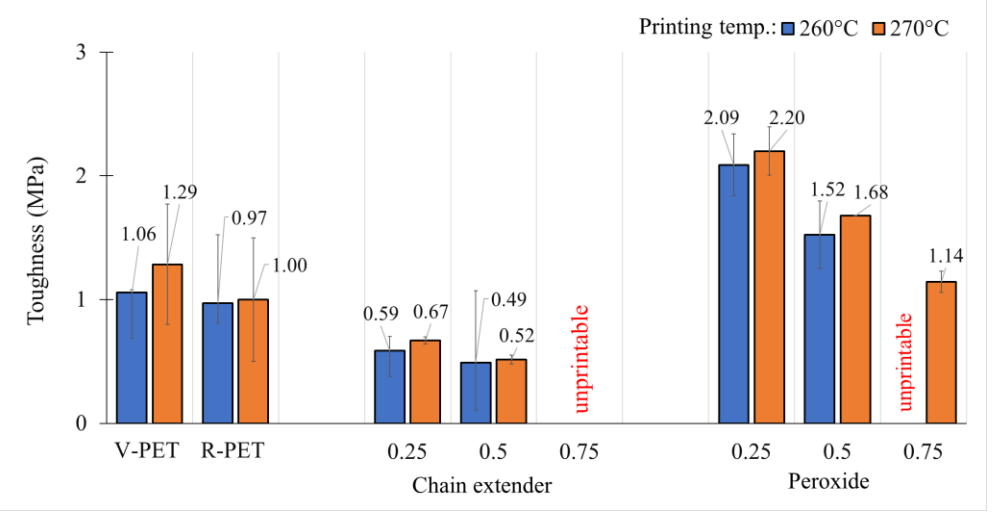

Fig. 13: Tensile toughness of all specimens at the printing temperatures of 260 ºC and 270 ºC and the bed temperature of 60 ºC.

toughness of all 3D-printed specimens was higher at the higher printing temperature due to lower filament viscosity and better adhesion between printed layers. Another parameter investigated here is the effect of heated bed temperature. An appropriate bed temperature is important for the shape stability of 3D-printed specimens as it could minimize the temperature gradient during the printing process. Here, the bed temperature was investigated at 60 ºC and 80 ºC at the ambient temperature of 29 ±1 ºC. The warpage angles of the 3D-printed specimens (4 specimens per sample) were measured, and the average values are shown with error bars in Fig. 14. As can be seen, the higher bed temperature resulted in a lower warpage angle indicating better shape stability overall. Nevertheless, when comparing among different filaments, it was found that peroxide provided a lower warpage angle and thus better shape stability than the neat and CE-modified R-PET. Since the warpage was reported to be more severe for polymers with higher molecular weight or higher degree of branching,[33] the lower warpage angle of peroxide-modified R-PETs might be due to their shorter chain (implied by lower zero-shear viscosity) and potentially lower degree of branching than the CE-treated R-PET. From all the results mentioned above, it can be concluded that peroxide at 0.25 wt% is an interesting additive to improve the quality of R-PET for the 3D-printing application as it could improve the toughness and shape stability of the 3D-printed specimen without compromising the lowest printable temperature. When comparing the performance of our modified R-PET with PLA and ABS, the modified R-PET exhibits a slightly higher T_g (76 ºC) than PLA (60 ºC) but lower than ABS (105 ºC), indicating better heat resistance than PLA but less than ABS. Given that the toughness of our modified R-PET is double that of V-PET, it is expected to surpass the toughness of both ABS and PLA, which have lower toughness than V-PET. To minimize warpage, our modified R-PET demands a lower bed temperature (80 ºC) than ABS (95-110 ºC) but slightly higher than PLA (60 ºC). Additionally, our modified R-PET offers significant advantages in terms of carbon footprint, cost-effectiveness, and the absence of toxic fumes associated with ABS. However, a downside of our modified R-PET is its higher printing temperature of 250-270 ºC, which exceeds that of ABS (240-260 ºC) and PLA (190-220 ºC).[34,35]

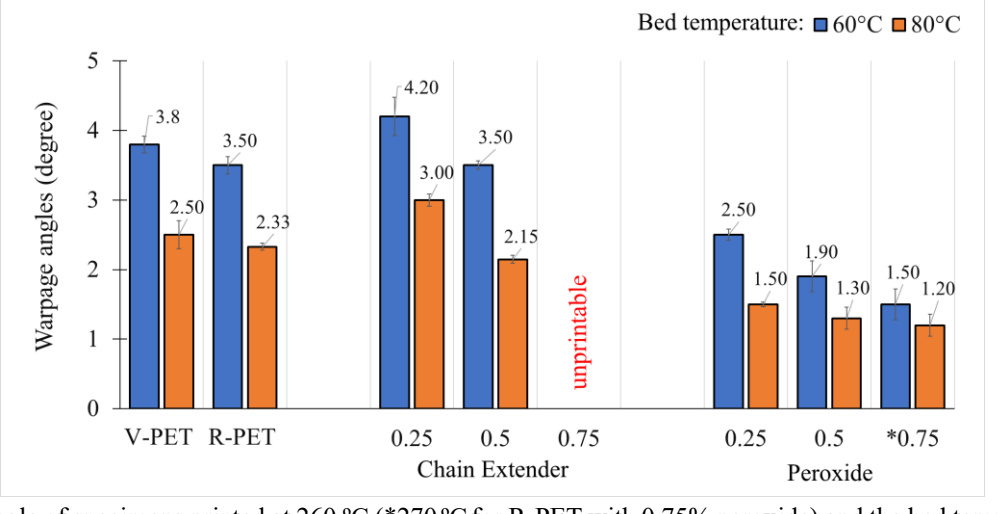

Fig. 14: Warpage angle of specimens printed at 260 ºC (*270 ºC for R-PET with 0.75% peroxide) and the bed temperatures of 60 and 80 ºC.

Furthermore, since our process of producing modified R-PET involves simple reactive compounding and requires only a small amount of nontoxic additive, it has high potential as a low-cost and low carbon-footprint 3D printing filament. Potential applications for our modified R-PET filaments include those requiring higher toughness, greater heat resistance, and lower costs compared to PLA. The main drawback is its higher printing temperature. In comparison to ABS, although ABS offers superior heat resistance and a lower printing temperature, our peroxide-modified R-PET provides higher toughness and allows for a lower bed temperature without creating a toxic printing environment. More importantly, it is made from a more environmentally friendly raw material.

Although peroxide-treated R-PET filaments provide significant environmental advantages and lower material costs, their successful utilization in 3D printing necessitates addressing quality control in PET waste collection. Lowering the printing temperature is another target for further development to enhance the competitiveness of R-PET filaments in the market.

4. Conclusion

In this work, R-PET retrieved from drinking water bottles was investigated for its potential as 3D-printing filaments for the material extrusion technique. The chemical structure of R-PET was improved by compounding with two different reactive additives, which were a multifunctional chain extender (CE) and a peroxide radical-initiator, by using a twin-screw extruder. It was found that the neat R-PET filament could be printed at a lower temperature (250 ºC) than the filament made from V-PET (260 ºC) with better shape stability but a slightly lower toughness. With the reactive modification, the addition of CE resulted in higher melt viscosity and storage modulus due to the formation of higher molecular weight, branching, and crosslinking. Conversely, the peroxide treatment tended to cause primarily chain scission together with a small degree of branching and crosslinking. Overall, peroxide treatment was more suitable for 3D printing than CE treatment because the viscosities of peroxide-modified R-PET filaments were sufficiently low, allowing them to be printed at the same temperature as neat R-PET (250 ºC). Additionally, it also provides the highest toughness, even surpassing those of V-PET. Properties of the 3D-printed specimens were further enhanced at a higher printing temperature of 270 ºC and the bed temperature of 80 ºC. The optimal peroxide content of 0.25 wt% resulted in specimens with a 35% reduction in warpage and 2.2 times higher tensile toughness compared to neat R-PET, achieving a warpage angle of 1.5° and a tensile toughness of 2.2 MPa.

Through simple reactive compounding with a small amount of a nontoxic additive like peroxide, our modified R-PET shows high potential as a low-cost and environmentally friendly 3D printing filament. Potential applications include those requiring higher toughness, better heat resistance, and lower costs compared to PLA but could accept a higher printing temperature (270 ºC). It can also be used for applications that does not demand as high heat resistance like ABS, but cheaper and potentially tougher without toxic emission during printing. Successful utilization of R-PET filaments in 3D printing requires quality control in PET waste collection and reduction of the printing temperature to enhance market competitiveness.

Acknowledgment

The authors gratefully acknowledge the Ph.D. scholarship from the Faculty of Engineering, Thammasat University, and additional support from the Research Unit in Polymer Rheology and Processing, Thammasat University.

Conflict of Interest

There is no conflict of interest.

Supporting Information

Not applicable.

References

[1] T. D. Ngo, A. Kashani, G. Imbalzano, K. T. Q. Nguyen, D. Hui, Additive manufacturing (3D printing): a review of materials, methods, applications and challenges, *Composites Part B: Engineering*, 2018, **143**, 172-196, doi: 10.1016/j.compositesb.2018.02.012.

[2] N. Shahrubudin, T. C. Lee, R. Ramlan, An overview on 3D printing technology: technological, materials, and applications, *Procedia Manufacturing*, 2019, **35**, 1286-1296, doi: 10.1016/j.promfg.2019.06.089.

[3] M. Alzahrani, H. Alhumade, L. Simon, K. Yetilmezsoy, C. M. R. Madhuranthakam, A. Elkamel, Additive manufacture of recycled poly(ethylene terephthalate) using pyromellitic dianhydride targeted for FDM 3D-printing applications, *Sustainability*, 2023, **15**, 5004, doi: 10.3390/su15065004.

[4] M. Leary, Chapter 8 - Material extrusion, In additive manufacturing materials and technologies, design for additive manufacturing, Elsevier B.V., Amsterdam, 2020, 223-268.

[5] N. E. Zander, M. Gillan, Z. Burckhard, F. Gardea, Recycled polypropylene blends as novel 3D printing materials, *Additive Manufacturing*, 2019, **25**, 122-130, doi: 10.1016/j.addma.2018.11.009.

[6] Z. Zhang, C. Wang, K. Mai, Reinforcement of recycled PET for mechanical properties of isotactic polypropylene, *Advanced Industrial and Engineering Polymer Research*, 2019, **2**, 69-76, doi: 10.1016/j.aiepr.2019.02.001.

[7] A. Dey, I. N. Roan Eagle, N. Yodo, A review on filament materials for fused filament fabrication, *Journal of Manufacturing and Materials Processing*, 2021, **5**, 69, doi: 10.3390/jmmp5030069.

[8] S. Yin, R. Tuladhar, F. Shi, R. A. Shanks, M. Combe, T. Collister, Mechanical reprocessing of polyolefin waste: a review, *Polymer Engineering & Science*, 2015, **55**, 2899-2909, doi:

10.1002/pen.24182.
[9] R. Daniele, D. Armoni, S. Dul, P. Alessandro, From nautical waste to additive manufacturing: sustainable recycling of high-density polyethylene for 3D printing applications, *Journal of Composites Science*, 2023, **7**, 320, doi: 10.3390/jcs7080320.
[10] J. Ahmed, A. Noon, A. Muhammad, M. Naveed, A. Khan, M. M. Suhaib, A. Sharif, Mechanical properties evaluation of recycled high-density polyethylene via additive manufacturing. *Journal of Materials and Manufacturing*, 2023, **2**, 1-9, doi: 10.5281/zenodo.10012303.
[11] A. Alassali, C. Picuno, Z. K. Chong, J. Guo, R. Maletz, K. Kuchta, Towards higher quality of recycled plastics: limitations from the material's perspective, *Sustainability*, 2021, **13**, 13266, doi: 10.3390/su132313266.
[12] M. R. Hasan, I. J. Davies, A. Pramanik, M. John, W. K. Biswas, Potential of recycled PLA in 3D printing: a review, *Sustainable Manufacturing and Service Economics*, 2024, **3**, 100020, doi: 10.1016/j.smse.2024.100020.
[13] D. Hidalgo-Carvajal, Á. H. Muñoz, J. J. Garrido-González, R. Carrasco-Gallego, V. Alcázar Montero, Recycled PLA for 3D printing: a comparison of recycled PLA filaments from waste of different origins after repeated cycles of extrusion, *Polymers*, 2023, **15**, 3651, doi: 10.3390/polym15173651.
[14] V. Mishra, C. K. Ror, S. Negi, S. Kar, L. N. Borah, 3D printing with recycled ABS resin: effect of blending and printing temperature, *Materials Chemistry and Physics*, 2023, **309**, 128317, doi: 10.1016/j.matchemphys.2023.128317.
[15] E. W. Hanitio, N. R. Lutfhyansyah, B. M. Efendi, Y. Mardiyati, S. Steven, From electronic waste to 3D-printed product, how multiple recycling affects high-impact polystyrene (HIPS) filament performances, *Materials*, 2023, **16**, 3412, doi: 10.3390/ma16093412.
[16] M. J. Reich, A. L. Woern, N. G. Tanikella, J. M. Pearce, Mechanical properties and applications of recycled polycarbonate particle material extrusion-based additive manufacturing, *Materials*, 2019, **12**, 1642, doi: 10.3390/ma12101642.
[17] F. Daver, R. Gupta, E. Kosior, Rheological characterisation of recycled poly(ethylene terephthalate) modified by reactive extrusion, *Journal of Materials Processing Technology*, 2008, **204**, 397-402, doi: 10.1016/j.jmatprotec.2007.11.090.
[18] L. Incarnato, P. Scarfato, L. Di Maio, D. Acierno, Structure and rheology of recycled PET modified by reactive extrusion, *Polymer*, 2000, **41**, 6825-6831, doi: 10.1016/S0032-3861(00)00032-X.
[19] M. Qu, D. Lu, H. Deng, Q. Wu, L. Han, Z. Xie, Y. Qin, D. W. Schubert, A comprehensive study on recycled and virgin PET melt-spun fibers modified by PMDA chain extender, *Materials Today Communications*, 2021, **29**, 103013, doi: 10.1016/j.mtcomm.2021.103013.
[20] X. Tang, W. Guo, G. Yin, B. Li, C. Wu, Reactive extrusion of recycled poly(ethylene terephthalate) with polycarbonate by addition of chain extender, *Journal of Applied Polymer Science*, 2007, **104**, 2602-2607, doi: 10.1002/app.24410.
[21] S. Japon, L. Boogh, Y. Leterrier, J. A. E. Månson, Reactive processing of poly(ethylene terephthalate) modified with multifunctional epoxy-based additives, *Polymer*, 2000, **41**, 5809-5818, doi: 10.1016/S0032-3861(99)00768-5.
[22] Z. Yang, C. Xin, W. Mughal, X. Li, Y. He, High-melt-elasticity poly(ethylene terephthalate) produced by reactive extrusion with a multi-functional epoxide for foaming, *Journal of Applied Polymer Science*, 2018, **135**, 45805, doi: 10.1002/app.45805.
[23] S. Makkam, W. Harnnarongchai, Rheological and mechanical properties of recycled PET modified by reactive extrusion, *Energy Procedia*, 2014, **56**, 547-553, doi: 10.1016/j.egypro.2014.07.191.
[24] I. N. A. Siriorn, B. Munchumart, B. Natanicha, S. Nut, M. Nopparat, H. Suchart, Viscosity improvement of recycled poly (ethylene terephthalate) from waste bottles by adding antioxidants and chain-extender, *E3S Web of Conferences*, 2021, **302**, 02019, doi: 10.1051/e3sconf/202130202019.
[25] D. Dimonie, R. Socoteanu, S. Pop, I. Fierascu, R. Fierascu, C. Petrea, C. Zaharia, M. Petrache, Overview on mechanical recycling by chain extension of POSTC-PET bottles, *Material Recycling - Trends and Perspectives*, 2012, 85-114, doi: 10.5772/31841.
[26] T. Standau, M. Nofar, D. Dörr, H. Ruckdäschel, V. Altstädt, A review on multifunctional epoxy-based joncryl® ADR chain extended thermoplastics, *Polymer Reviews*, 2022, **62**, 296-350, doi: 10.1080/15583724.2021.1918710.
[27] C. Fosse, A. Bourdet, E. Ernault, A. Esposito, N. Delpouve, L. Delbreilh, S. Thiyagarajan, R. J. I. Knoop, E. Dargent, Determination of the equilibrium enthalpy of melting of two-phase semi-crystalline polymers by fast scanning calorimetry, *Thermochimica Acta*, 2019, **677**, 67-78, doi: 10.1016/j.tca.2019.03.035.
[28] G. C. Berry, T. G. Fox, The viscosity of polymers and their concentrated solutions, Fortschritte der Hochpolymeren-Forschung, Berlin/Heidelberg: Springer-Verlag, 2006, 261-357, doi: 10.1007/bfb0050985.
[29] C. Pattamaprom, R. G. Larson, T. J. Van Dyke, Quantitative predictions of linear viscoelastic rheological properties of entangled polymers, *Rheologica Acta*, 2000, **39**, 517-531, doi: 10.1007/s003970000104.
[30] S. T. Milner, T. C. B. McLeish, Reptation and contour-length fluctuations in melts of linear polymers, *Physical Review Letters*, 1998, **81**, 725-728, doi: 10.1103/physrevlett.81.725.
[31] C. Pattamaprom, R. G. Larson, Predicting the linear viscoelastic properties of monodisperse and polydisperse polystyrenes and polyethylenes, *Rheologica Acta*, 2001, **40**, 516-532, doi: 10.1007/s003970100196.
[32] A. R. Payne, The dynamic properties of carbon black-loaded natural rubber vulcanizates. Part I, *Journal of Applied Polymer Science*, 1962, **6**, 57-63, doi: 10.1002/app.1962.070061906.
[33] F. Khabaz, R. Khare, Effect of chain architecture on the size, shape, and intrinsic viscosity of chains in polymer solutions: a molecular simulation study, *The Journal of Chemical Physics*, 2014, **141**, 214904, doi: 10.1063/1.4902052.
[34] E. Bezeraj, S. Debrie, F. J. Arraez, P. Reyes, P. H. Van

Steenberge, D. R. D'hooge, M. Edeleva, State-of-the-art of industrial PET mechanical recycling: technologies, impact of contamination and guidelines for decision-making. RSC Sustainability, 2025, **3**, 1996-2047, doi: 10.1039/D4SU00571F.
[35] S. Ding, B. F. Ng, X. Shang, H. Liu, X. Lu, M. P. Wan, The characteristics and formation mechanisms of emissions from thermal decomposition of 3D printer polymer filaments, *Science of the Total Environment*, 2019, **692**, 984-994, doi: 10.1016/j.scitotenv.2019.07.257.